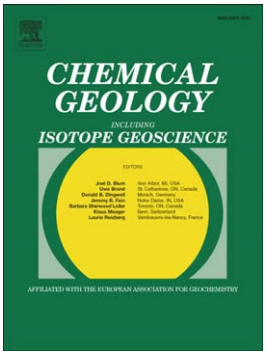

Experimental mixing of hydrous magmas

Mickael Laumonier, Bruno Scaillet, Laurent Arbaret, Joan Andújar, Rémi Champallier

PII: S0009-2541(15)30078-4
DOI: doi: 10.1016/j.chemgeo.2015.10.031
Reference: CHEMGE 17740

To appear in: *Chemical Geology*

Received date: 11 February 2015
Revised date: 24 August 2015
Accepted date: 20 October 2015

Please cite this article as: Laumonier, Mickael, Scaillet, Bruno, Arbaret, Laurent, Andújar, Joan, Champallier, Rémi, Experimental mixing of hydrous magmas, *Chemical Geology* (2015), doi: 10.1016/j.chemgeo.2015.10.031

EXPERIMENTAL MIXING OF HYDROUS MAGMAS

Mickael LAUMONIER[1,2,3], Bruno SCAILLET[1,2,3], Laurent ARBARET[1,2,3], Joan ANDÚJAR[1,2,3], Rémi CHAMPALLIER[1,2,3]

[1]Univ d'Orléans, ISTO, UMR 7327, 45071, Orléans, France

[2] CNRS/INSU, ISTO, UMR 7327, 45071 Orléans, France

[3] BRGM, ISTO, UMR 7327, BP 36009, 45060 Orléans, France

Corresponding author: M. LAUMONIER

mickael.laumonier@gmail.com

ABSTRACT

Deformation experiments involving hydrous magmas of different compositions (basalt and haplotonalite) have been performed in a Paterson press at 300 MPa, in the temperature range 600°C-1020°C, with water-saturated melts, during 2-4 hours. Prior to deformation the two end-member magmas were annealed at either 950°C or 1000°C, yielding magmas with crystal contents in the range 31-53 wt% and 2 sets of viscosity contrasts. Under the experimental conditions investigated (i.e. moderate shear rates $<10^{-3}$ s^{-1}), mixing/mingling textures appear at temperatures > 950°C. In the temperature range 950-985°C a few mixing and mingling textures occur, though both end-members essentially retain their physical integrity. It is only at, or above, 1000°C that a dramatic jump in mingling efficiency happens, corresponding to a crystal fraction of 45 vol%. Textures include entrainment of mafic crystals into the felsic magma, mafic-felsic banding, enclave formation, diffusion-induced interface, the latter only

over limited distances (< 300 microns) due to the short run durations. In the most strained parcels of interacting magmas, complex mixing/mingling textures were produced, similar to those observed in volcanic and plutonic rocks in arc settings. The experiments show that mixing between hydrous felsic and mafic magmas takes place at around 1000°C, a temperature which is almost 200°C lower than mixing under dry conditions. Magma mixing is commonly invoked as a trigger for volcanic eruptions; our experiments suggest that such eruptions can be driven by small (~15°C) temperature fluctuation in the reservoir. Our results also suggest that slow replenishment of a felsic reservoir by mafic inputs will likely result in stratification between end-members rather than in a homogeneous mixture.

KEY WORDS:

Magma mixing; mingling; hydrous; shearing; deformation; texture; enclave

1. INTRODUCTION

Magma mixing is commonly observed in nature, in particular in arc magmas, which are characterised by an abundance in volatiles, notably water (Anderson, 1976; Armienti et al., 1983; Blake, 1984; Castro et al., 1990; Coombs et al., 2002; De Rosa et al., 1996; Druitt et al., 1999; Martin et al., 2006a,b; Pons et al., 2006; Pal et al., 2007; Woods & Cowan, 2009; Davì et al., 2010; Eichelberger 2010; Perugini & Poli, 2012). The effects of mixing are particularly evident when evolved magma chambers stored at upper crustal pressures ($P < 400$ MPa) are replenished by batches of hot (up to 1250°C) and mafic magmas (e.g. Sparks et al., 1977; Sakuyama, 1979; 1981; Bacon, 1986; Civetta et al., 1991; Nakamura, 1995; Pallister et al., 1996; Mandeville et al., 1996; Wiebe, 1996; Venezky & Rutherford, 1997; Clynne, 1999; Miller et al., 1999; Browne et al., 2006; Pal et al., 2007; Eichelberger, 2010; Ruprecht & Bachmann, 2010). Magma mixing has an important role in the dynamics of the processes occurring in magmatic reservoirs and it has been proposed as a triggering mechanism of volcanic eruptions (e.g., Sparks et al., 1977; Pallister et al., 1996; Eichelberger, 2010; Kent et al., 2010; Ruprecht & Bachmann, 2010; La Felice & Landi, 2011; Druitt et al., 2012). Mixing depends on the rheological properties of magmas that are in turn strongly affected by volatiles. In particular, dissolved water strongly decreases melt viscosity (Dingwell et al., 1996), affects the fraction of crystals present at a given temperature, which, in turn, affects magma viscosity (Champallier et al., 2008; Caricchi et al., 2007; Picard et al., 2011). Consequently water and volatiles, in general, strongly influence magma behavior and eruptive style, depending on whether the magma holds or loses its volatiles during its transfer to surface (e.g., Jaupart & Allègre, 1991; Martel et al., 1998; Laumonier et al., 2011). However, dynamic experiments designed to explore magma mixing processes at the water-rich conditions found in arc settings in particular are absent (Kouchi & Sunagawa, 1982; 1985; Watson & Jurewicz, 1984; Wyllie et al., 1989; Carroll & Wyllie, 1989; van der Laan & Wyllie, 1993; De Campos et al., 2008; 2011). So far, most works have been conducted at

atmospheric pressure (i.e. using dry magmas), high temperature (1200 to 1400°C), under static conditions or at high strain rates (~10^{2} s^{-1} by Kouchi & Sunagawa, 1982; 1985; ~10^{-1} s^{-1} by De Campos et al., 2008; 2011; and ~10^{-2} s^{-1} by Morgavi et al., 2013a; 2013b). Such conditions, in particular strain rate, are consistent with volcanic eruption processes, but exceed those characteristic of magma reservoirs prior to eruption (10^{-4} s^{-1}, Chadwick et al., 1988; Albertz et al., 2005; Hodge et al., 2012). Recently, Laumonier et al. (2014a) deformed two chemically distinct and dry magmas at conditions close to expected magmatic ones, i.e. 900 < T < 1200°C, 300 MPa and strain rate of 10^{-5} to 10^{-3} s^{-1}. The geometry used imposes simple shear at the interface between the two end-members, to simulate replenishment of a reservoir by a mafic dyke intrusion (Fig. 1A). These dry experiments reproduce most of the textures of magma mixing and mingling observed in rocks (enclaves, stretched filament, isolated crystal in disequilibrium with their host), clarifying the details of the mechanisms occurring during the incipient stages of mixing. The fraction and the arrangement of crystals appears to be a critical factor for magma mixing, in particular via the existence of crystal network, which controls the magma rheology (e.g., Philpotts et al., 1998; Martin et al., 2006a; Laumonier et al., 2014a; Caricchi et al., 2012). However, the dry conditions explored by Laumonier et al. were aimed at limiting quench effects, to better document mixing textures and related mechanisms. Here, we extend our efforts toward hydrous conditions using a methodology similar to that in Laumonier et al. (2014a). To the best of our knowledge this is the first time that the effect of water on the mixing capacity of magmas is experimentally investigated under conditions of temperature, pressure, and strain rate relevant to subduction zone settings.

2. EXPERIMENTAL PROCEDURE

2.1. Starting material

A natural basalt and a synthetic haplotonalite were selected as the mafic and felsic end-members for torsion experiments, allowing a direct comparison with previous dry experiments (Laumonier et al., 2014a). The basalt (composition in Table 1) was sampled from the massive part of the Cape Balos flow on Santorini volcano, Greece (Nicholls, 1971; Druitt et al., 1999). It contains phenocrysts of olivine (Fo75) that are set in a matrix of plagioclase, clinopyroxene, magnetite with rare ilmenite and orthopyroxene. Xenocrysts of olivine (Fo_{78}) and plagioclase (An_{90}) are also present, the latter sometimes displaying core sieved textures and inverse compositional zoning (cores: An55-60, rims An80) (Nicholls, 1971; Andújar et al., 2015). The phase equilibria of the mafic material have been investigated by Andujar et al. (2015) and are used as a guideline for our work. The haplotonalitic glass (Table 1) was produced by Schott A.G. (Germany). In the P-T-H_2O range explored it crystallizes plagioclase only and the relationships between crystal fraction, water content, and temperature have been previously determined (Picard, 2009; Picard et al., 2011; Laumonier et al., 2011). The chemical and rheological behaviors of such a plagioclase suspension in a felsic glass are similar to natural felsic magmas (trachyte to rhyolite, e.g. Calanchi et al., 1993; Ferla & Meli, 2006; Davi et al., 2010).

These two starting materials were first hydrated and annealed in an Internally Heat Pressure Vessel (IHPV) at 300 MPa and 950 or 1000°C, depending on the target crystal fraction. The felsic magmas synthesized at 950°C and 1000°C have crystal contents (Φs) of 38 and 31 vol.% respectively, with ~10 µm long plagioclase (An29 to An35) having an aspect ratio of 2-3, along with a few percent of bubbles (<2% in volume) and glass (Fig. 2A; Table 1). The mafic syntheses contain 53 vol% (at 950°C) and 45 vol % (at 1000°C) of amphibole + plagioclase + pyroxene + magnetite and glass (Fig. 2C & D, Table 1). More details about the preparation and syntheses can be found in the supplementary information.

2.2. Deformation experiments

2.2.1. *Experimental set up for deformation experiments*

Cylinders from first step synthesis products were drilled out (13.78 to 14.96 mm diameter) and cut into thin disks (1.16 to 3.34 mm thick) to build the experimental torsion assembly while some pieces from different locations in the syntheses were selected to check the suspension homogeneity. Our deformation set up consists of 4 interleaved wafers of felsic/mafic magma synthesized at the same temperature and alternating in composition, always with a felsic disk located atop of the "stack" (Fig. 1B). Layers are named according to their position and composition, e.g. numbering from the top, and ρ and β symbols for felsic and mafic compositions, respectively (Fig. 1B). In all experiments except the run conducted at the lowest temperature (3 layers: ρ1, β2 and ρ3), the upper layer was ρ1 and the lower one is β4 providing 3 interfaces between end-members. The faces of each disk were ground to have parallel sides (thickness variation lower than 0.02 mm) and polished to reduce interface irregularities. The stack of disks (5.33 to 10.93 mm thick) was wrapped in a platinum foil, which did not significantly chemically interact with the sample during the experiments. This assemblage was inserted in turn in a copper or iron jacket and sandwiched between pistons to be located in the isothermal zone of the furnace (± 2°C on 35 mm length determined during furnace calibration). Although in nature strong thermal gradients likely exist between mixing magmas, in this study we tried to avoid any temperature gradient to better constrain the role of melt fraction on mixing. Our experiments hence model the conditions of mixing once thermal equilibrium has been reached between the end-members. The column so prepared was inserted in a Paterson press (Paterson instrument, Australian Scientific Instruments) at ISTO to perform torsion experiments at constant strain rate. Such a deformation configuration reproduces simple shear conditions and allows the deformation of one material only without forcing the whole stack to deform, such as happening during the replenishment of a felsic

reservoir by a mafic dyke (Fig. 1; *e.g.* Castro, 1987). During preliminary tests, we used a different sample geometry consisting of two half cylinders, one mafic and one felsic, sharing a vertical interface. However such a geometry was not mechanically sustainable, the rapid collapse of the less viscous material imparting an off-axis rotation of the entire column which could lead to severe damages of the apparatus: hence it was not used any further.

2.2.2. *Experimental conditions*

Seven torsion, and one static experiments were performed at 300 MPa, in the temperature interval 600-1020°C (Table 2). The prevailing oxygen fugacity was measured with a Shaw membrane during a calibration experiment and found to be 1 log unit above the Nickel-Nickel oxide solid buffer ($fO_2 \approx$ NNO+1±0.5) (Scaillet et al. 1992). Torsion was applied during 1 to 4 hours at strain rates $2.10^{-4} < \dot{\gamma} < 9.10^{-4}$ s^{-1} allowing to achieve relatively large finite strains ($0.7 < \gamma < 5.1$). Most torsion experiments were performed in the temperature range 950°C-1020°C, with an iron jacket (Table 2). Torsion experiments started by the pressurization of the vessel up to ~220 MPa, followed by heating which permits to reach the final pressure (300 MPa). Mixing experiments were performed using starting materials whose synthesis temperature was the closest to that of the deformation experiment (Table 2). The temperature difference relative to that of the synthesis may induce melting (PP262, PP293 & PP295, Table 2) or crystallization (PP258, PP265 & PP296), during the 1-hour lap time allowed before torsion was applied. The lap time of low temperature experiments (600°C and 715°C) lasted 15 minutes so as to minimize crystallization. Torsion was applied until jacket failure was noticed by the drop of the load applied on the column holding the sample and experiments were ended by an isobaric quench (~60°C/mn). Additional details on the experimental set-up and techniques can be found in Paterson & Olgaard (2000).

After experiments, samples were recovered and embedded in epoxy resin for textural observation and chemical microanalyses. Generally, the initial geometry of each layer is well preserved, no significant compaction or vertical shrinkage was noticed (see lengths before and after experiments, determined from SEM pictures, Table 2). Observations were made on tangential sections far enough from the sample periphery to avoid interferences resulting from the jacket deformation (see details in supplementary information). The textural and chemical results of the four experiments characterizing the transition from non-mixing to mixing conditions are detailed (950-1000°C; Table 2).

3. RESULTS

3.1. Strain distribution and macroscopic observations

During torsion experiments the jacket that moulds the sample is also affected by the deformation (Paterson & Olgaard, 2000). Thus, the local strain distribution along sample length (affecting each layer) can be directly inferred by photo reconstruction and image analysis of the outer jacket (Fig. 3). Whenever the strain is not homogeneously distributed across the stack, the deflection of vertical linear markers on the jacket, together with standard trigonometric relationships, are used to determine the local strain distribution (Fig. 3). The quantification of the local strain was confirmed by calculations based on the twisting angle and the sample dimension (Paterson & Olgaard, 2000).

While experiments conducted at subsolidus temperature exhibit a strong partitioning of the deformation, the ones above 950°C display deformational textures generally affecting both layers (Fig. 3). In detail, SEM pictures show that the felsic material, also being less viscous, still preferentially accommodated the strain until 985°C (Fig. 4A-C). In contrast, at T > 1000°C, abundant mingling features such as irregular interfaces between end-members, boudinage and mafic enclaves (in the sense of aggregates of mafic minerals) in the felsic

magma were produced, despite a relatively low strain γ_{bulk} < 1.3 (Fig. 4D & E). In those experiments conducted at T > 1000°C, both end-members were clearly deformed, in agreement with the near homogeneous strain distribution observed on the jacket (Fig. 3D).

Lastly, two of the seven experiments (PP295 and PP261) were affected by extrusions of material through holes in the jacket (Fig. 3B & D). Although such extrusions were uncontrolled they shed light on mingling and mixing features produced at higher strain (supplementary information).

3.2. Microscopical observations

3.2.1. *Phase proportions*

The crystal content was determined by SEM-image analysis of areas in mafic layers that were close to the felsic component and having a surface > 0.8 mm² to avoid local heterogeneities. Textural analyses concerning the PP261 experiment were performed over a smaller area (0.35 mm²) for the enclave and farther from the contact because of the interface complexity (see below). While the experiments conducted at low temperature (600 and 715°C) have a phase assemblage and proportions similar to the starting material (Fig. 2C & 5A; Table 1), felsic and mafic layers in experiments conducted at T>950°C display considerable textural changes relative to starting products, in particular a higher crystal content in both magmas, as a result of quench crystallization. For instance, the melt fraction in mafic layers decreased from 48-58 to 24-32 vol.% (Fig. 5A). The experiment conducted at 985°C (grey squares on Figure 5) has the lowest melt fraction as a result of a large increase in plagioclase proportion, more than 4 times the starting values (Fig. 5B). Olivine occurs in all experiments at 950°C or higher temperature (up to 3% in volume). Oxides are generally absent, but occasionally observed (e.g. PP261, PP285). In felsic layers the crystal fraction is similar to that of the corresponding synthesis at low temperature (715°C), but increases in all run products annealed at higher

temperatures, up to 65 vol.% in the products of PP296. No dependence of the melt/crystal fraction with temperature, duration or finite strain of the experiment could be established. Changes in crystal fraction in the felsic layers also result from diffusion at the interface, more or less affected by deformation.

3.2.2. *Textures*

In the run products of PP285 (950°C), PP295 (975°C) and PP296 (985°C), interfaces are no more straight but wavy (dashed line labeled 1, Fig. 6A to C). Despite their regular and nearly cylindrical shape, mafic layers underwent little deformation. A few single plagioclase and pyroxene crystals coming from the mafic layers are found in the felsic one (yellow arrow on Figure 6A). The SPO intensity defined by plagioclase in the felsic layers is low (<1.02) except in the experiment PP296 that suffered a high bulk strain. Crystal fractions of synthesis experiments are no longer preserved: the plagioclase population in the felsic layers is denser close to the mafic layer creating a halo 50 µm (PP285) to 270 µm (PP296) thick (dashed line labeled 2, Fig. 6), with crystal fractions up to 65%, whereas areas farther from mafic layers contain 47% of plagioclase.

Despite the relatively low amount of deformation reached in the experiments at 1000 and 1020°C (respectively γ=1.3 and γ=0.7), interfaces between end-members are also characterized by embayments and lobes at the scale of tens of µm (Fig. 6D). Wavy contacts are accompanied by isolated crystals and parcels of mafic magma, hereafter called “mafic enclaves”, the latter having rounded shape and sizes ranging from tens of µm (aggregates constituted of a few crystals) up to 1 mm (Fig. 6D & E). Enclaves have a texture similar to the inner mafic layer one. Around the enclave presented in Figure 6E, a light SPO developed in the felsic layer made of 49% plagioclase, with intensities of 1.03 and 1.04, coinciding with the direction of the interface between the enclave and its host (Fig. 6E). The poorly developed

SPO of plagioclases around the enclave in the felsic layer supports the localization of the deformation instead of the development of a pervasive fabric.

3.3. Compositions of phases

Unfortunately, the extensive quench crystallization affecting the run products severely complicates the interpretation of compositional data, in particular melt, hence obscuring their possible implications for natural contexts. For this reason we limited data acquisition essentially to the analyses of crystals in run products obtained at 1000°C considering the following domains or textures:

-“β>500”: inner parts of mafic layers, relatively far (500 µm minimum) from the contact with the felsic component. Such parts are likely to have had little to no interactions with the felsic component;

-“β<150”: external parts of the mafic layers, at 150 µm maximum from the contact;

-“interface”: such as the layer bridging the boudins (Fig. 6D) or that close to the lobe (Fig. 6D, F);

-“enclave”: the enclave (in the sense of rounded crystals aggregate) produced in the PP261 experiment (Fig. 5E);

-“isolated”: crystals located in the felsic layer with a composition and a texture different from the typical plagioclase population crystallizing from the haplotonalitic liquid.

-“ρ>300”: concerns only the plagioclases in the felsic end-member at a distance >300 µm from any mafic layer and may be compared with the composition of plagioclase from the felsic synthesis (Htn). The phases from torsion experiments are compared with those from the 1000°C synthesis and the static experiment also conducted at 1000°C.

3.3.1. *Plagioclase*

Plagioclase cores are similar to the plagioclase in the starting suspension (An80-An92) whereas rims are more sodic with An50-An76 (Fig. 7A). Plagioclases produced in the static experiment systematically developed a rim wherever they are located in the mafic layer. In general, plagioclases from torsion experiments are similar, with a large rim (An39-An77) to core (An79-An93) zonation. Analyzed plagioclases located within the mafic layers (β>500) have a rim that extends to An44, slightly less calcic than those from the mafic inner parts (β>500) of the static experiment (An50). In contrast, rims of crystals close to felsic component (β<150µm; An37-An77) and non zoned acicular crystals located in the interface layer (An40-An67, Fig. 7A) have compositions less calcic than those in the residual mafic melt. Such acicular plagioclases are larger when located close to the mafic layer. The smallest ones occur close to the felsic component and could not be analyzed because of their size. Some plagioclases having similar size and aspect ratio to those from the mafic layer do also occur in the interface layer, with an anorthite content typical of the core composition (An82-An93). Theses plagioclases are frequently surrounded by acicular crystals, whose occurrence makes difficult the analysis of the thin rim overgrowth. Isolated large plagioclases in the haplotonalite, presumably from the mafic component, are also zoned with a calcic core composition (An79-An90) and a sodic rim (An40). Plagioclases with a typical felsic composition (~An35) were only observed within the felsic layer (ρ>300).

3.3.2. *Olivine*

Olivine, which is absent from the starting syntheses performed in conventional IHPV, is present in both static and torsion experiments conducted in the Paterson Press (Table 1). In the static experiment, olivine has a Fo content ranging between Fo70 and Fo77 (Fig. 7B). The olivines of torsion experiments display a larger Fo content variation, especially in the mafic

areas close to the felsic component (Fo64-Fo81 in β<150 areas). Olivines within the interface layer, from enclaves or isolated, display a more restricted variability in Fo (Fo75-80), though Fo is not higher than in β<150 areas, from where they might be sourced (Fig. 7B).

3.3.3. *Pyroxene*

The composition of pyroxene is shown in Fig. 7C. Pyroxenes from the static experiment have a composition similar to those from the starting mafic suspension when they are located within the mafic layer (β>500), whereas close to the haplotonalite (β<150) their composition varies along a trend with constant Ferrosilite ≈ 12%, and varying Ca and Mg contents (Fig. 7C) though changes in En and Wo contents remain small. In torsion experiments, most pyroxenes have a composition quite similar to the starting pyroxenes (Fig. 7C). Pyroxenes from the interface layers, enclaves, the inner (β>500) and the outer (β<150) parts of the mafic layers, also roughly follow the Fs = 0.12 trend (Ca concentration ranging between 32 and 47 molar %).

3.3.4. *Glass*

Glass analyses of static and torsion experiments reveal SiO_2 contents ranging between 55 and 69 wt% (Fig. 8), falling between the SiO_2 content of the starting glasses, though some analyses are more mafic. In contrast, the CaO concentration ranges between 2.6 and 8.2 wt.%, which plot slightly above the trend between both end-members (Fig. 8). Most melt analyses located in the external parts of the mafic layers (β<150) and within enclaves have compositions slightly more evolved than the starting mafic one (higher SiO_2 and lower CaO content). In contrast, melt pockets between acicular crystals of the interface layer display heterogeneous melt compositions (SiO_2 ranging from 56 to 68 wt.%; Fig. 8).

4. DISCUSSION

4.1. General considerations

The textures produced in the torsion experiments record, in part, the incipient stages of mafic-felsic interaction processes when the shearing deformation is parallel to the interface at relatively low strain rates, once the thermal equilibrium has been reached. As already stated, this scenario reproduces the local deformation pattern happening during the replenishment of a reservoir when a magma rises through dykes in a reservoir, though experimental strain rates might also be applicable to some volcanic processes (Castro, 1987; Albertz et al., 2005; Chadwick et al., 1988; Fig. 1A). Although we do not claim that our experiments reproduce faithfully all processes happening during magma mixing, we believe that they likely mimic the incipient stage of mixing at a microscale in natural hydrous magmas.

Due to faster kinetics resulting from the high water content (e.g. Dingwell et al., 1996), the cooling rate of the vessel could not prevent the development of quench crystals whose occurrence partly obscures textural observations. Interpretation of experimental products is based on the first step syntheses that were ended by a drop quench, hence allowing better preservation of the HP/HT phase proportions. Although attention was paid to the development of fabric with applied strain, quench effects are too severe to extract any useful information in this field, as well as for the quantification of mixing intensity. The fact that plagioclase fabrics of the felsic layers are nearly isotropic (Fig. 5) should be viewed as a direct consequence of crystallisation during cooling in an almost isotropic stress field. Only in the lowest temperature experiments (600°C-700°C) does the fabric record the effect of deformation, showing that under the investigated conditions the mafic magma is unaffected, while plagioclases in the felsic magma are re-oriented at the vicinity of the contact with the mafic layer (Supplementary materials).

The presence of olivine and oxide in torsion products most likely reflects changes in the prevailing oxygen fugacity, as other parameters (T, P, H_2O) were kept constant. Experimental work performed on the Balos basalt from Santorini supports this observation: at NNO+3.5 and water-saturated conditions olivine is not stable whereas magnetite + clinopyroxene or magnetite + clinopyroxene + amphibole predominate at ≥1000ºC and 950ºC, respectively (Andújar et al., 2015). In contrast, at NNO, the stable mineral assemblage is olivine + clinopyroxene + plagioclase ± magnetite for temperatures > 985ºC; and amphibole co-crystallizes with these phases in the range 985-975ºC (Andújar et al., 2015). Thus, the occurrence of olivine in torsion experiments records the lower fO_2 conditions in the Paterson experiments relative to those prevailing in synthesis experiments, but without significantly changing the crystal fraction (Andújar et al., 2015).

4.2. Interpretation of chemical results

Chemical data reflect interactions produced during the experiments, *i.e.* from the 1-hour lap time before deformation to the cooling of the experiment. The diffusion distance of the main elements anticipated from the application of the diffusivity laws is consistent with what is observed in run products; for instance, the self diffusivity of Mg is about 10^{-8} to 10^{-9} cm²/s in hydrous felsic melts (van der Laan & Wyllie, 1993; Mungall et al., 1999; Zhang et al., 2010) and the expected diffusion distance after 2 hours is ~90 to ~360 µm (calculated using the relationships $x = (Dt)^{1/2}$, x being distance in m, D diffusivity in m^2/s and t time in s), in agreement with the chemical halo highlighted by elemental mapping (supplementary information) which extends over 200 µm at higher temperature (1000°C, PP261). Similarly, the expected distances by self diffusion of Ca (10^{-8} to 2.10^{-7} cm²/s) after 2 hours are 260 to 520 µm (van der Laan & Wyllie, 1993; Watson, 1981; Zhang et al., 2010). Therefore, assuming that the presence of crystals does not affect diffusion properties, chemical mixing occurring prior to deformation is likely to have been affected by strain.

There are no significant compositional differences between clinopyroxenes crystallizing under either static or dynamic conditions whereas plagioclase and olivine define larger compositional intervals (Fig. 7), which may reflect the effect of mixing but also that of quench. Similar compositions of crystals whatever their localisation indicate efficient crystal-melt separation compared to the timescale of chemical equilibration. In static experiments olivine composition is Fo77-Fo70 and plagioclase is An80-An50 whilst in related torsion experiments, olivine and plagioclase compositions extend towards lower Mg (Fo64) and Ca (An40) values, suggesting that deformation enhances mixing process, probably via the entrainment of mafic minerals into felsic liquids. This is also supported by the wide compositional diversity of liquids which are sometimes more mafic than those obtained under synthesis conditions (Fig. 8). Clearly, however, it is also on liquid compositions that quench effects are maximised, which calls for caution in interpreting experimental trends solely in terms of mixing processes. Owing to profuse quench effects, chemical inferences from our experiments are necessarily very limited, though in agreement with observations made on dry compositions (Laumonier et al., 2014a), which show that the stacked, contrasted magmas produces a range of phase compositions, either solids or liquids. This is despite the relatively short run durations, < 4 hours. A large range of compositions has been also observed in previous experimental studies simulating mixing under static conditions (e.g., Johnston & Wyllie, 1988).

4.3. Effect of water on mixing

4.3.1. *Development of mingling/mixing features in hydrous magmas*

The hydrous experiments described here document the progressive development of mingling and mixing textures over a 50°C temperature interval (under our experimental conditions). The first mingling feature appears at 950°C and corresponds to the mechanical

incorporation of isolated mafic crystals into the felsic magma (Fig. 6B), such as pyroxene and calcic plagioclase (An80-An92). When immersed in the felsic component, isolated plagioclases developed a sodic rim (An40 to An70), producing a normal zoning pattern (Fig. 6 & 7). This contrasts with isolated plagioclases observed in dry conditions, characterized by resorption features and poorly developed rim (Laumonier et al., 2014a). At 950°C and higher temperatures, diffusion operates and can be observed in the felsic layers: the crystallization of plagioclase with more calcic composition around mafic layers results from the diffusion of calcium from the mafic component (Fig. 6). The effective diffusion of Fe and/or Mg is also marked by the halo of tiny Fe-Mg minerals in the PP296 experiment (Fig. 6C). The PP296 experiment can be compared to the PP156 run of Laumonier et al. (2014a): both lack mingling textures, despite being just 10-15°C below the temperature at which profuse mixing/mingling textures were produced. However, diffusion has clearly occurred in the hydrous experiment. Therefore, water allows mixing to operate even at temperatures slightly below the crystal rheological threshold (~0.50).

At 975 and 985°C, interface instabilities are generated (Fig. 6B & C) but the mafic layers still maintain their cylindrical shape in spite of a relatively high finite strain (γ = 5.1, PP296, Fig. 4). The first clear change in layer shape is observed in the runs performed at T>1000°C where both end-members are folded and stretched to boudin-like geometries, presumably because of the collapse of the touching crystal network. Hence, it appears that, at crystal fractions lower than 45%, mafic layers dislocate and produce enclaves, larger-scale lobes and embayments (e.g. Hodge et al., 2012).

4.3.2. *Origin of diktytaxitic textures*

The presence of acicular microcrystals within the margins of enclaves is often interpreted as resulting from fast cooling of the hotter mafic enclave in its cold host (e.g. Bacon, 1986; Gerbe & Thouret, 2004; Troll et al. 2004; Martin et al., 2006b; Davì et al.,

2010). Such a fast crystallization leads to volatile exsolution and resulting bubbles which are entrapped within the crystals network, forming diktytaxitic texture (Fig. 6F & Fig. 9A). However, our experimental observations offer an alternative explanation: they suggest that the rim composed of crystals in many enclaves is not the result of a fast cooling only, but may come from the existence of a chemical gradient in the transition zone. As shown in dry experiments, the interface between chemically contrasted magmas is subject to chemical reactions (Laumonier et al., 2014a). Our hydrous experiments also produced a layer composed of plagioclase (fraction ~0.35), amphibole (~0.20), inherited pyroxenes (0.05) and dacitic melt (0.40). Most amphiboles and plagioclases in the layer are acicular but they are relatively large, approaching the size of crystals of the starting material (Fig. 6G), which suggest that they have started to grow before the quench, reflecting crystallization at P and T. The absence of such a rim around the enclave produced in PP261 can be explained by the fact that chemical diffusion was erased by higher local strain, in spite of a Mg-enriched haplotonalite halo (Fig. S2). A chemical gradient between two hydrous magmas was also the cause of the development of a reaction zone such as reported by Johnston & Wyllie (1988). In these experiments, a change in clinopyroxene composition with respect to its position to the interface was reported. Carroll & Wyllie (1989) also produced a reaction layer in their hydrous experiments between peridotite and granite at 1050 °C and 1.5 GPa, consisting of small pyroxenes. The weak chemical variation observed in clinopyroxenes in our experiments is possibly the result of the deformation, favoring the interaction zone and thus enhancing homogenization. Therefore, chemical gradients between enclaves and their magma host may play a role on the development of rims, which is not limited to the chilling effect of a hot mafic blob. Textural features from enclaves from Soufrière Hills supports such an hypothesis (Fig. 9); the external parts of a basaltic-andesitic enclave contain significantly more amphiboles, and a halo of plagioclases separates the enclave from the andesitic host,

resembling the amphibole and plagioclase layers produced in our experiments (Fig. 6F & 11B). The orientation of the amphiboles at the periphery of the enclave is not perpendicular to the contact, but roughly parallel to it, indicating that some flow occurred after their crystallization. Therefore, amphibole is more likely to result from a chemical transition rather than from a quench process only. According to our results, such a texture is possible at a relatively low crystal fraction, which is consistent with the abundance of melt in both the enclave and its host.

4.3.3. *Importance of the crystal fraction and viscosity contrast*

The comparison with the dry experiments of Laumonier et al. (2014a) shows that the presence of water decreases the temperature at which magma mixing and mingling happens by 170°C; the widespread mafic magma remobilization indeed sets in suddenly at 1000°C, as compared to 1170°C under dry conditions. Such a difference is close to the one between the liquidus temperature between hydrous and dry basaltic magmas (Andùjar et al., 2015). Water shifts down the liquidus temperature, thus the crystallisation and consequently magma mixing capacities. Our experiments are thus in agreement with the concept of a rheological threshold, as proposed by e.g. Philppots et al. (1998) and Martin et al (2006a) and more recently by Laumonier et al. (2014a). The onset of dismembering of the whole mafic layer occurs between 985 and 1000°C, corresponding to a crystal fraction close to 45% and similar to mixing experiments at dry conditions (Laumonier et al., 2014a). At 985°C and lower temperatures, the crystal fraction is high enough to build a rigid (touching) crystal network controlling the mush rheology that even strain cannot break at our experimental conditions. A modest temperature rise of 15°C results in the diminution of the crystal fraction, allowing the dismembering of the crystal network and subsequent magma mingling. However, in detail, a few minor and discrete mingling textures (isolated crystals, crenulated contact) do occur before the onset of large scale dislocation of the mafic layers, such as in the charge at 950°C

(Fig. 6A), establishing a more progressive transition between mixed and unmixed magmas than that observed under dry conditions. Such a progressive transition might result in the lower melt viscosity under hydrous conditions.

At subsolidus tempertures (600 and 715°C), the viscosity contrast between the mafic and felsic melts does not exceed 0.3 log unit (Laumonier et al.; 2014b). However, neither mingling nor mixing features were produced in those conditions. In fact, the viscosity contrast between magmas (melt plus crystals) is about 1 log unit, which seems large enough to prevent mixing (under our deformation conditions), as observed under dry conditions (Laumonier et al., 2014a). Therefore, our results support the important role of the crystal fraction, which controls bulk viscosity, on the remobilization and mixing of dry and hydrous magmas. Within the range of strain rates explored here, a difference in the viscosities of interacting magmas (either hydrous or dry) of about an order of magnitude is enough to prevent them from being mixed.

Lastly, the material extruded out of the samples during PP261 and PP295 experiments bears texturally complex mingling/mixing features (see supplementary materials). Although strain, strain rate and also the deformation geometry cannot be precisely determined, the other parameters (in particular T) are similar to those reigning in the sample. The PP295 experiment conducted at 975°C shows that the rheological transition has been upset in the case of extrusions: there, the crystal network hindering magma mingling in the interior sample was locally broken by a different regime of deformation when the magma was extruded through a hole in the jacket, creating filament and rounded shape textures. On this basis it can be concluded that mixing processes are considerably enhanced by elevated rates of deformations (compare Fig. 4 and Fig. S2), as found in other experimental studies or by a particular geometry of the interface forcing both magmas to be deformed (e.g. De Campos et al., 2011 ; Morgavi et al., 2013a, b). The textures produced in the extrusions are similar to those

observed in the main samples at T>1000°C (PP261 & PP293) but better developed, presumably as a result of the high strain underwent by the magma (also including the production of stretched filaments; Fig. S2). Hence, we suggest that a relatively high crystal fraction (~0.50) may not be adequate to mixing and mingling in magma reservoir, but still feasible (until a certain fraction) in the volcanic conduit where higher strain and strain rate occur or in highly dynamic reservoirs where convective rates allow high strain rates to be attained (Woods & Cowan, 2009; Pritchard et al., 2013).

4.4. Implications for reservoir replenishments

In the light of these results we suggest that reservoirs being slowly replenished will have less possibility to produce well-mixed magmas, in accord with the results of analogical experiments (e.g. Turner & Campbell, 1986; Jellinek et al., 1999; Hodge et al., 2012). Strain rates in convecting reservoirs are inferred to be quite low, $<10^{-6}$ s^{-1} (e.g., Spera et al., 1988; Albertz et al., 2005) which therefore suggests that mixing between rheologically contrasted magmas (i.e. with viscosities differing by more than 1 order of magnitude) are unlikely to be efficient at this location. In contrast, mixing during vigorous, or forcefull, injection may lead to thoroughly mixed material or hybrids, as illustrated by the extrusions and experiments involving natural basalt and rhyolite differing in viscosity by ~ 4 orders of magnitude, which nevertheless were mingled and mixed at higher temperature (T>1350°C) and strain rates (~10^{-2} s^{-1}; De Campos et al., 2011; Morgavi et al., 2013a, 2013b). Considering that the P-T-H_2O conditions investigated here cover those likely to prevail in most arc magmas reservoirs (Scaillet et al., 1998; Andújar and Scaillet, 2012), our experiments constrain the temperature at which mixing can operate. As a general rule, our results suggest that injection of a mafic forerunner into a crystal-rich silicic host will not produce hybrid products if the equilibration temperature of the blended mixture remains below 950°C. The final temperature of equilibration depends, *inter alia*, on the relative masses of interacting end-members (Sparks

and Marshall, 1986; Frost and Mahood, 1987; Laumonier et al., 2014b) and so there is no unique solution to this problem. However, it can be anticipated that the slow replenishment via small mafic inputs of a large felsic reservoir, will not give rise to prolonged and widespread thermal excursions, and hence will lead to conditions unfavourable to mixing: slow replenishment will more likely end up producing stratified intrusions rather than a homogeneous whole body. Consequently, we suggest that mixing features encountered in highly crystallized magmas (> 50% crystals) may have been produced before their crystallization (closer to liquidus conditions, Scaillet et al., 2000; Caricchi et al., 2012) or in extreme strain rate environments such as in volcanic conduits where the strain rates, during eruption, exceed the average plutonic ones (e.g., Koyaguchi & Blake, 1989; Pritchard et al., 2013). That the mixing efficiency changes rapidly over a small temperature interval suggests in turn that small temperature variations may give rise to abrupt changes in the fluid dynamics of injected reservoirs. Eruptions triggered by mafic inputs may thus record the case of felsic reservoirs lying close to the rheological threshold prior to mafic injection.

5. CONCLUSION

We present the results of the first experiments on mixing and mingling of hydrous magmas performed at P-T-H_2O conditions relevant to arc contexts (P = 300 MPa, T < 1020°C and water contents up to 6.5 wt.% in the melt). Our low strain rate torsion experiments on hydrated wafers of felsic/mafic magmas fully reproduce the mingling textures observed in natural magmas (isolated crystals, boudin-like structures, enclaves) and mixing textures like the development of chemical halo and transition layers. Such layers consist of a dense population of plagioclase, and acicular crystals, melt and bubbles, altogether resembling the diktytaxitic texture often observed in natural enclave margins that may result from the rapid crystallization of a chemical transition between magmas. Mixing and mingling of hydrous magmas appears feasible at low crystal fraction (< 50 vol.%) and low viscosity contrast

(within one order of magnitude), and at temperatures shifted by ~200°C when compared to similar but dry magmas (Laumonier et al., 2014a). Finally, the transition between mixing and unmixing regimes appears more progressive in water-bearing magmas. However, mingling can occur at crystal fractions higher than the critical crystallinity, in particular under extreme strain rate conditions. Those conditions prevail in volcanic conduits, suggesting that mixing involving highly crystallized magmas may be the consequence of volcanic eruptions.

FUNDING

This work was supported by the French Agence National de Recherche [ANR-08CEA080 to B. S], and Equipex PLANEX.

ACKOWLEDGEMENTS

We greatly thank I. Di Carlo for analytical support and E. Lemoing and P. Teulat for technical assistance. The reviews of K. Russel, M. Pistone and an anonymous reviewer helped in focusing the topic of this manuscript. We are also grateful to K. Mezger and the guest editors of this special issue for editorial assistance.

REFERENCES

Albertz, M., Paterson, S.R., Okaya, D. (2005). Fast strain rates pluton emplacement: Magmatically folded leucocratic dikes in aureoles of the Mount Stuart Batholith, Washington, and the Tuolumne Intrusive Suite, California, *Geological Society of America Bulletin* **117**, 450-465.

Anderson, A.T. (1976). Magma mixing: petrological process and volcanological tool, *Journal of Volcanology and Geothermal Research* **1**, 3-33, doi:10.1016/0377-0273(76)90016-0.

Andújar, J., Scaillet, B. (2012). Relationships between pre-eruptive conditions and eruptive styles of phonolites-trachyte magmas. *Lithos*, doi:10.1013/j.lithos.2012.05.009.

Andújar, J., Scaillet, B., Druitt, T.H., Pichavant, M. (2015). Differentiation conditions of a basaltic magma from Santorini, and its bearing on the production of andesite in arc settings. *Journal of Petrology* **56**, 765-794.

Armienti, P., Barberi, F., Bizouard, H., Clocchiatti, R., Innocenti, F., Metrich, N., Rosi, M., Sbrana, A. (1983). The phlegraean fields: Magma evolution within a shallow chamber. *Journal of Volcanology and Geothermal Research* **17** (1-4), 289-311, DOI: 10.1016/0377-0273(83)90073-2.

Bacon, C. R. (1986). Magmatic Inclusions in Silicic and Intermediate Volcanic Rocks. *Journal of Geophysical Research* **91** (B6), 6091–6112, doi:10.1029/JB091iB06p06091.

Barnhoorn, A., Bystricky, M., Kunze, K., Burlini, L., Burg, J.P. (2005). Strain localization in bimineralic rocks: Experimental deformation of synthetic calcite-anhydrite aggregates. *Earth and Planetary Science Letters* **240**, 748-763.

Berndt, J., Koepke, J., Holtz, F. (2005). An experimental investigation of the influence of water and oxygen fugacity on differentiation of MORB at 200 MPa. *Journal of Petrology* **46**, 135-167.

Blake, S. (1984). Magma mixing and hybridization processes at the alkalic, silicic, Torfajokull central volcano triggered by tholeiitic Veidivotn fissuring, south Iceland. *Journal of Volcanology and Geothermal Research* **22** (1-2), 1-31, DOI: 10.1016/0377-0273(84)90033-7.

Blundy, J.D., Sparks, R.S.J. (1992). Petrogenesis of mafic inclusions in granitoids of the Adamello Massif, Italy, *Journal of Petrology* **33**, 1039-1104.

Browne, B.L., Eichelberger, J.C., Patino, L.C., Vogel, T.A., Uto, K., Hoshizumi, H. (2006). Magma mingling as indicated by texture and Sr / Ba ratios of plagioclase phenocrysts from Unzen volcano, SW Japan. *Journal of Volcanology and Geothermal Research* **154** (1-2) 103-116, DOI: 10.1016/j.jvolgeores.2005.09.022.

Calanchi, N., De Rosa, R., Mazzuoli, R., Rossi, P., Santacroce, R., Ventura, G. (1993). Silicic magma entering a basaltic magma chamber: eruptive dynamics and magma mixing — an example from Salina (Aeolian islands, Southern Tyrrhenian Sea). *Bulletin of Volcanology* **55** (7), 504-522.

Caricchi, L., Burlini, L., Ulmer, P., Gerya, T., Vassalli, M., Papale, P. (2007). Non-Newtonian rheology of crystal-bearing magmas and implications for magma ascent dynamics. *Earth and Planetary Science Letters* **264**, 402-419.

Caricchi, L., C. Annen, A. Rust, and J. Blundy, 2012, Insights into the mechanisms and timescales of pluton assembly from deformation patterns of mafic enclaves: Journal of Geophysical Research, doi:10.1029/2012JB009325.

Carroll, M., Wyllie, P.J. (1989). Granite melt convecting in an experimental micro-magma chamber at 1050°C, 15 kbar. *European Journal of Mineralogy* **1**, 249-260.

Castro, A. (1987). On granitoid emplacement and related structures. A review, *Geologische Rundschau* **76**, 101-124 (Springer).

Castro, A., De La Rosa, J.D., Stephens, W.E. (1990). Magma mixing in the subvolcanic environment: petrology of the Gerena interaction zone near Seville, Spain. *Contributions to Mineralogy and Petrology* **106**, 9-26, Doi:10.1007/BF00306405.

Chadwick, W.W., Archuleta, R.J., Swanson, D.A., 1988. The mechanics of ground deformation precursory to dome-building extrusions at Mt. St. Helens 1981–1982. *Journal of Geophysical Research* **93**, 4351–4366.

Champallier, R., Bystricky, M., Arbaret, L. (2008). Experimental investigation of magma rheology at 300MPa: From pure hydrous melt to 76 vol.% of crystals. *Earth and Planetary Science Letters* **267** (3-4), 571-583.

Civetta, L., Galati, R., Santacroce, R. (1991). Magma mixing and convective compositional layering within the Vesuvius magma chamber. *Bulletin of Volcanology* **53** (4), 287-300, DOI: 10.1007/BF00414525.

Clynne, M.A. (1999). A Complex Magma Mixing Origin for Rocks Erupted in 1915, Lassen Peak, California. *Journal of Petrology* **40** (1), 105-132, doi: 10.1093/petroj/40.1.105.

Coombs, M.C., Eichelberger, J.C., Rutherford, M.J. (2002). Experimental and textural constraints in mafic enclave formation in volcanic rocks. *Journal of Volcanology and Geothermal Research* **119**, 125-144, doi:10.1016/S0377-0273(02)00309-8

Davi, M., De Rosa, R., Holtz, F. (2010). Mafic enclaves in the rhyolitic products of Lipari historical eruptions; relationships with the coeval Vulcano magmas (Aeolian Islands, Italy). *Bulletin of Volcanology* **72** (8), 991-1008, DOI: 10.1007/s00445-010-0376-5.

De Campos, C.P., Dingwell, D.B, Perugini, D., Civetta, L., Fehr, T.K. (2008). Heterogeneities in magma chambers: Insights from the behavior of major and minor elements during mixing experiments with natural alkaline melts. *Chemical Geology* **256**, 131-145.

De Campos, C.P., Perugini, D., Ertel-Ingrisch, W., Dingwell, D.B., Poli, G. (2011). Enhancement of magma mixing efficiency by chaotic dynamics :an experimental study. *Contributions to Mineralogy and Petrology* **161**, 863-881.

De Rosa, R., Mazzuoli, R., Ventura, G. (1996). Relationships between deformation and mixing processes in lava flows: a case study from Salina (Aeolian Islands, Tyrrhenian Sea). *Bulletin of Volcanology* **58**, 286-297, DOI: 10.1007/s004450050140.

Dingwell, D.B., Romano, C., Hess, K.U. (1996). The effect of water on the viscosity of a haplogranitic melt under P-T-X conditions relevant to silicic volcanism. *Contribution to Mineralogy and Petrology* **124**, 19-28.

Druitt, T.H., Edwards, L., Mellors, R.M., Pyle, D.M., Sparks, R.S.J., Lanphere, M., Davies, M., Barriero, B. (1999). Santorini Volcano. *Journal of Geological Society of London*, Memoir 19, pp165.

Druitt, T.H., Costa, F., Deloule, E., Dungan, M., Scaillet, B. (2012). Decadal to monthly timescales of magma transfer and reservoir growth at a caldera volcano., *Nature* **482**, 77-80.

Eichelberger, J.C. (2010). Messy magma mixtures. *Nature Geoscience* **3**, 593-594, doi:10.1038/ngeo951.

Ferla, P., Meli, C. (2006). Evidence of magma mixing in the 'Daly Gap' of alkaline suites: a case study from the enclaves of Pantelleria (Italy). *Journal of Petrology* **47**, 1467-1507.

Frost, T.P., Mahood, G.A. (1987). Field, chemical, and physical constraints on mafic-felsic magma interaction in the Lamarck Granodiorite, Sierra Nevada, California. *Geological society of America Bulletin* **99**, 272-291.

Gerbe, M.C., Thouret, J.C. (2004). Role of magma mixing in the petrogenesis of tephra erupted during the 1990–98 explosive activity of Nevado Sabancaya, southern Peru. *Bulletin of Volcanology* **66**, 541-561.

Giordano, D., Russell, J.K., and Dingwell, D.B. (2008). Viscosity of magmatic liquids: A model. *Earth and Planetary Science Letters* **271** (1-4), 123–134, doi: 10.1016/j.epsl.2008.03.038.

Hodge, K. F., G. Carazzo, and A. M. Jellinek, 2012, Experimental constraints on the deformation and breakup of injected magma: Earth and Planetary Science Letters, v. 325-326, p. 52–62, doi:10.1016/j.epsl.2012.01.031.

Jaupart, C., Allègre, C. (1991). Gas content, eruption rate and instabilities of eruption regime in silicic volcanoes. *Earth and Planetary Science Letters* **102**, 413-429.

Johnston, A.D., Wyllie, P.J. (1988). Interaction of granitic and basic magmas: experimental observations on contamination processes at 10 kbar with H_2O. *Contribution to Mineralogy and Petrology* **98**, 352-362.

Kent, A.J.R, Darr, C., Koleszar, A.M., Salisburry, M.J., Cooper, K.M. (2010). Preferential eruption of andesitic magmas through recharge filtering. *Nature Geoscience* **3**, 631-636.

Kouchi, A., Sunagawa, I., (1982). Experimental study of mixing of basaltic and dacitic magmas,.*Science Reports of the Tohoku University*, ser. 3, vol. **15**, 163-175.

Kouchi, A., Sunagawa, I. (1985). A model for mixing basaltic and dacitic magmas as deduced from experimental data. *Contributions to Mineralogy and Petrology* **89**, 17–23, DOI: 10.1007/BF01177586.

Koyaguchi, T., Blake, S. (1989). The dynamics of magma mixing in a rising magma batch. *Bulletin of Volcanology* **52**, 127–137, DOI: 10.1007/BF00301552.

La Felice, S., Landi, P. (2011). The 2009 paroxysmal explosions at Strombolie (Italy): magma mixing and eruption dynamics. *Bulletin of Volcanology* **73**, 1147-1154.

Laumonier, M., Arbaret, L., Burgisser, A., Champallier, R. (2011). Porosity redistribution enhanced by strain localization in crystal-rich magmas. *Geology* **39** (8), 715-718.

Laumonier, M., Scaillet, B., Arbaret, L., & Champallier, R. (2014a). Experimental simulation of magma mixing at high pressure. *Lithos **196***, 281-300.

Laumonier, M., Scaillet, B., Pichavant, M., Champallier, R., Andújar, J., & Arbaret, L. (2014b). On the conditions of magma mixing and its bearing on andesite production in the crust. *Nature communications **5***, doi:10.1038/ncomms6607.

Mandeville, C.W., Carey, S., Sigurdsson, H. (1996). Magma mixing, fractional crystallization and volatile degassing during the 1883 eruption of Krakatau volcano, Indonesia. Journal of Volcanology and Geothermal Research 74 (3-4), 243-274, DOI: 10.1016/S0377-0273(96)00060-1.

Martel, C., Pichavant, M., Bourdier, J.L., Traineau, H., Holtz, F., Scaillet, B. (1998). Magma storage conditions and control of eruption regime in silicic volcanoes: experimental evidence from Mt. Pelee. *Earth and Planetary Science Letters* **156**, 89-99.

Martin, V.M., Holness, M.B., Pyle, D.M. (2006a). The role of crystal frameworks in the preservation of enclaves during magma mixing. *Earth and Planetary Science Letters* **248**, 787-799.

Martin, V.M., Holness, M.B., Pyle, D.M. (2006b). Textural analysis of magmatic enclaves from the Kameni Islands, Santorini, Greece. *Journal of Volcanology and Geothermal Research* **154** (1-2), 89-102, DOI:10.1016/j.jvolgeores.2005.09.021.

Miller, T.P., Chertkoff, D.G., Eichelberger, J.C., Coombs, M.L. (1999). Mount Dutton Volcano, Alaska: Aleutian Arc analog to Unzen volcano, Japan. *Journal of Volcanology and Geothermal Research* **89**, 275-302.

Morgavi, D., Perugini, D., De Campos, C.P., Ertel-Ingrish, W., Lavallée, Y, Morgan, L., Dingwell, D.B. (2013a). Interactions between rhyolitic and basaltic melts unraveled by chaotic mixing experiments, *Chemical Geology* **346**, 199-212.

Morgavi, D., Perugini, D., De Campos, C.P., Ertel-Ingrish, W., Dingwell, D.B. (2013b). Time evolution of chemical exchanges during mixing of rhyolitic and basaltic melts, *Contribution to Mineralogy and Petrology* **166**, 615-638.

Morimoto, N., Fabries, J., Ferguson, A.K., Ginzburg, I.V., Ross, M., Seifert, F.A., Zussman, J., Aoki, K., Gottardi, G. (1988). Nomenclature of Pyroxenes. *American Mineralogist* **73**, 1123-1133.

Mungall, J. E., Dingwell, D. B., & Chaussidon, M. (1999). Chemical diffusivities of 18 trace elements in granitoid melts. *Geochimica et cosmochimica acta*, *63*(17), 2599-2610.

Nakamura, M. (1995). Continuous mixing of crystal mush and replenished magma in the ongoing Unzen eruption. *Geology* **23**, 807–810, doi: 10.1130/0091-7613.

Nicholls, I. A. (1971). Petrology of Santorini Volcano, Cyclades, Greece. *Journal of Petrology* **12** (1), 67-11

Pal, T., Mitra, S.K., Sengupta, S., Katari, A., Bandopadhyay, P.C., Bhattacharya, A.K. (2007). Dacite-andesite of Narcondam volcano in the Andaman sea – An imprint of magma mixing in the inner arc of the Andaman-Java subduction system. *Journal of Volcanology and Geothermal Research* **168**, 93-113, doi:10.1016/j.jvolgeores.2007.08.005.

Pallister, J.S., Hoblitt, R.P., Meeker, G.P., Knight, R.J., and Siems, D.F. (1996). Magma mixing at Mount Pinatubo: Petrographic and chemical evidence from 1991 deposits, in Newhall, C., and Punongbayan, R., eds., Fire and Mud: Eruptions and Lahars of Mount Pinatubo: Quezon City, Philippine Institute of Volcanology and Seismology, and Seattle, University of Washington Press, 687-732.

Paterson, M., Olgaard, D. (2000). Rock deformation tests to large shear stress in torsion. *Journal of Structural Geology* **22**, 1341-1358, doi:10.1016/S0191-8141(00)00042-0.

Perugini, D., Poli, G. (2012). The mixing of magmas in plutonic and volcanic environment:Anologies and differences. *Lithos*, DOI:10.1016/j.lithos.2012.02.002.

Philpotts, A.R., Shi, J., Brustman, C. (1998). Role of plagioclase crytal chains in the differentiation of partly crystallized basaltic magma. *Nature* **395**, 343-346.

Picard, D. (2009). HP-HT deformation of silicic magmas: experimental constrains on the structural evolution and the rheological threshold at middle and high crystallinities, PhD thesis, University of Orleans (FR), pp.334.

Picard, D., Arbaret, L., Picahvant, M., Champallier, R., Launeau, P. (2011). Rheology and microstructures of experimentally plagioclase suspensions. *Geology* **39**, 747-750.

Pons, J., Barbey, P., Nachit, H., Burg, J.P. (2006). Development of Igneous layering during growth of pluton: the Tarçouate Laccolith (Morocco). *Tectonophysics* **413**, 271-286.

Pritchard, C. J., Larson, P. B., Spell, T. L., Tarbert, K. D. (2013). Eruption-triggered mixeing of extra-caldera basalt and rhyolite complexes along the East Gallatin-Washburn fault zone, Yellowston National Park, WY, USA. *Lithos* **175-176**, 163-177.

Ruprecht, P., Bachmann, O. (2010). Pre-eruptive reheating during magma mixing at Quizapu volcano and the implications for the explosiveness of silicic arc volcano. *Geology* **38** (10), 919-922, doi:10.1130/G31110.1.

Sakuyama, M. (1979). Evidence of magma mixing: petrological study of Shirouma-Oike calc-alkaline andesite volcano, Japan. *Journal of volcology and Geothermal research* **5**, 179-208, doi:10.1016/0377-0273(79)90040-4.

Sakuyama, M. (1981). Petrological study of the Myoko and Kurohime volcanoes, Japan: Crystallization sequence and evidence for magma mixing. *Journal of Petrology* **22** (4), 553-583.

Scaillet, B., Pichavant, M., Roux, J., Humbert, G. & Lefevre, A. (1992). Improvements of the Shaw membrane technique for measurement and control of fH2 at high temperatures and pressures. *American Mineralogist* **77**, 647–655.

Scaillet, B., Holtz, F., Pichavant, M. (1998). Phase equilibrium constraints on the viscosity of silicic magmas, 1. Volcanic-plutonic comparison. *Journal of Geophysical research* **103** (B11), 27257-27266.

Scaillet, B., Whittington, A., Martel, C., Picahvant, M., Holtz, F. (2000). Phase equilibrium constraints on the viscosity of silicic magmas with implications for mafic-silicic mixing processes. Transactions of the Royal Society of Edinburgh: earth Sciences **91**, 61-72.

Sparks, S.R.J., Sigurdsson, H., and Wilson, L. (1977). Magma mixing: A mechanism for triggering acid explosive eruptions. Nature **267** (5609) 315-318, doi: 10.1038/267315a0.

Sparks, R.S.J., Marshall, L.A. (1986). Thermal and mechanical constraints on mixing between mafic and silicic magmas. Journal of Volcanology and Geothermal Research **29**, 99–124, doi:10.1016/0377-0273(86)90041-7.

Spera, F.J., Borgia, A., Strimple, J., Feigenson, M., (1988). Rheology of melts and magmatic suspensions. 1. Design and calibration of a concentric cylinder viscometer for application to rhyolitic magma. J. Geophys. Res. 93, 10273-10294.

Troll, V.R., Donaldson, C.H., Emeleus, C.H. (2004). Pre-eruptive magma mixing in ash-flow deposits of the tertiary Rum Igneous Centre, Scotland. Contribution to Mineralogy and Petrology **147**, 722-739.

Turner, J.S., Campbell, I.H. (1986). Convection and Mixing in Magma Chambers, Earth-science reviews **23**, 255-352.

Van der Laan, S.R., Wyllie, P.J. (1993). Experimental interaction of granitic and basaltic magmas and implications for mafic enclaves. *Journal of Petrology* **34**, 491-517.

Venezky, D.Y., Rutherford, M.J. (1997). Preeruption conditions and timing of dacite-andesite magma mixing in the 2.2 ka eruption at Mount Rainier. *Journal of Geophysical Research* **102** (B9), 20,069-20,086, doi:10.1029/97JB01590

Watson, E. B. (1981). Diffusion in magmas at depth in the Earth: The effects of pressure and dissolved H_2O. *Earth and Planetary Science Letters*, *52*(2), 291-301.

Watson, E.B., Jurewicz, S.R. (1984). Behavior of alkalies during diffusive interaction of granitic xenoliths with basaltic magma. *Journal of Geology* **92**, 121-131.

Wiebe, R.A. (1996). Mafic-silicic layered intrusions: The role of basaltic injections on magmatic processes and the evolution of silicic chambers. *Royal Society of Edinburgh Transactions, Earth Sciences* **87**, 233-242.

Woods, A.W., Cowan, A. (2009). Magma mixing triggered during volcanic eruptions. *Earth and Planetary Science Letters* **288** (1-2) 132-137, DOI: 10.1016/j.epsl.2009.09.015.

Wyllie, P.J., Carroll, M.R., Johnston, A.D., Rutter, M.J., Sekine, T., Van der Laan, S.R. (1989). Interactions among magmas and rocks in subduction zone regions: experimental studies from slab to mantle to crust. *European Journal of Mineralogy* **1**, 165-179

Zhang, Y., Ni, H., & Chen, Y. (2010). Diffusion data in silicate melts. *Reviews in Mineralogy and Geochemistry*, *72*(1), 311-408.

FIGURE CAPTIONS

Figure 1: Shear deformation occurring during reservoir replenishment and reproduced in torsion experiments. (A) Simple shear may occur between a rising dyke or propagating sill of mafic magma within a felsic intrusion at relatively high shear rate (10^{-5} to 10^{-2} s^{-1}; Albertz et al., 2005). (B) Stack of sample geometry used for static and torsion experiments. The colours grey and black refer to the felsic and the mafic end-members, respectively. The black arrows indicate the sense of shearing.

Figure 2: SEM picture of starting synthetic suspensions of haplotonalite (felsic) and basalt (mafic), synthesized at 950°C and 1000°C. The felsic suspensions include melt (m), plagioclase (Pl) and bubbles (Bb) while the mafic suspensions are composed of melt, plagioclase, amphibole (Amp), clinopyroxene (Px), magnetite oxide (Ox), and bubbles. Φs is the crystal fraction of the suspension. The initial Shape Preferred Orientation of the felsic suspensions has been determined and the ellipsoid of the fabric is indicated with the long axis orientation and the intensity i of the SPO. The bar scale represents 100µm. See the text for phase proportions and details.

Figure 3: Reconstructed panorama of deformed samples still embedded in their jacket. Stack and relative layer thicknesses are indicated on the left side. Strain markers have been highlighted by a white line, dashed when not visible. The strain distribution is homogeneous at T > 950°C (see also Fig. S5). Experiments conducted at 975 and 1000°C (B & D) produced extrusions out of the jacket, in which mafic (m) and felsic (f) materials are visible.

Figure 4: SEM pictures of large sections showing the relative position of layers after torsion experiments. The scale bar on the bottom left corner represents 2 mm. A sketch of the layer

position is drawn on the right side. The sense of shear presented in (A) is common to all sections. Note that panels D is relatively close to the periphery of the sample, and might display features resulting from the effects of simple shear and the local deformation of the jacket.

Figure 5: (A) Phase proportions of the mafic layers. (B) Phase proportions for the area comprised between 0 and 150 µm from the contact with the felsic magma, normalized to the 950 and 1000°C phase proportions of the static mafic layers. The olivine fraction in (B) could not be calculated due to its absence in the starting suspension.

Figure 6: Details on particular textures produced in torsion experiments (see Fig. 4 for localization). Same crystal legend as Figure 1a, and Ol stands for olivine. The scale bar on the bottom left corner represents 100µm and the sense of shear presented in (A) is the same in all sections. Close to mafic layer, plagioclase crystals of the felsic layer are highlighted by white segments (A) and reveal the Shape Preferred Orientation developed at the interface, within the felsic layer. Local crystal fraction (percentages) and shape preferred orientation (ellipsoid and SPO intensity) were analysed on areas corresponding to the pictures. Dashed lines 1, 2 and 3 surround the mafic layer, the plagioclase-rich and ferromagnesian + plagioclase-rich layers, respectively. White arrows show isolated crystals mechanically extracted from the mafic layer in (B) and enclaves in (I). Arrows in (F & H) show bubble trails. Abbreviations are: m:melt, Pl:plagioclase, Bb:bubbles, Amp:amphibole, Px: clinopyroxene, Ox: magnetite oxide. See text for further details.

Figure 7: Molar anorthite content of plagioclase in 1000°C and “reheated” Syntheses, static and torsion experiments. Mg# of olivine (B) and pyroxene (C, after classification of Morimoto et al, 1988) in experimental products. See the text for mineral provenance.

Figure 8: CaO vs. SiO_2 wt.% of glasses from syntheses, static and torsion experiment.

Figure 9: Natural examples of magma mixing from (A) Adamello Massif (Blundy and Sparks, 1992), (B) Lipari products (Davì et al., 2010) and Montserrat Hills Volcano (C).

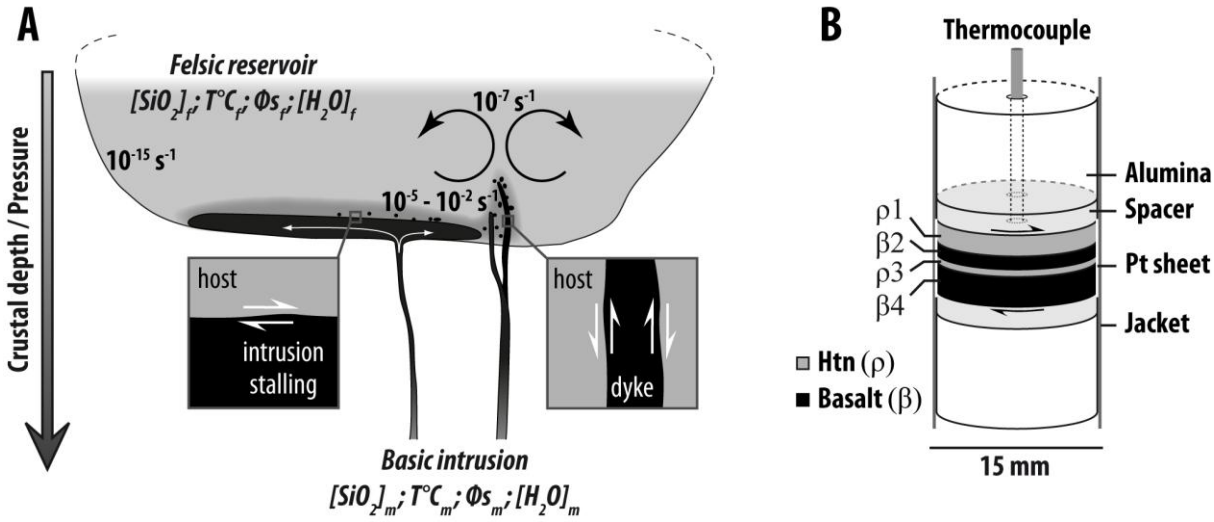

Fig. 1

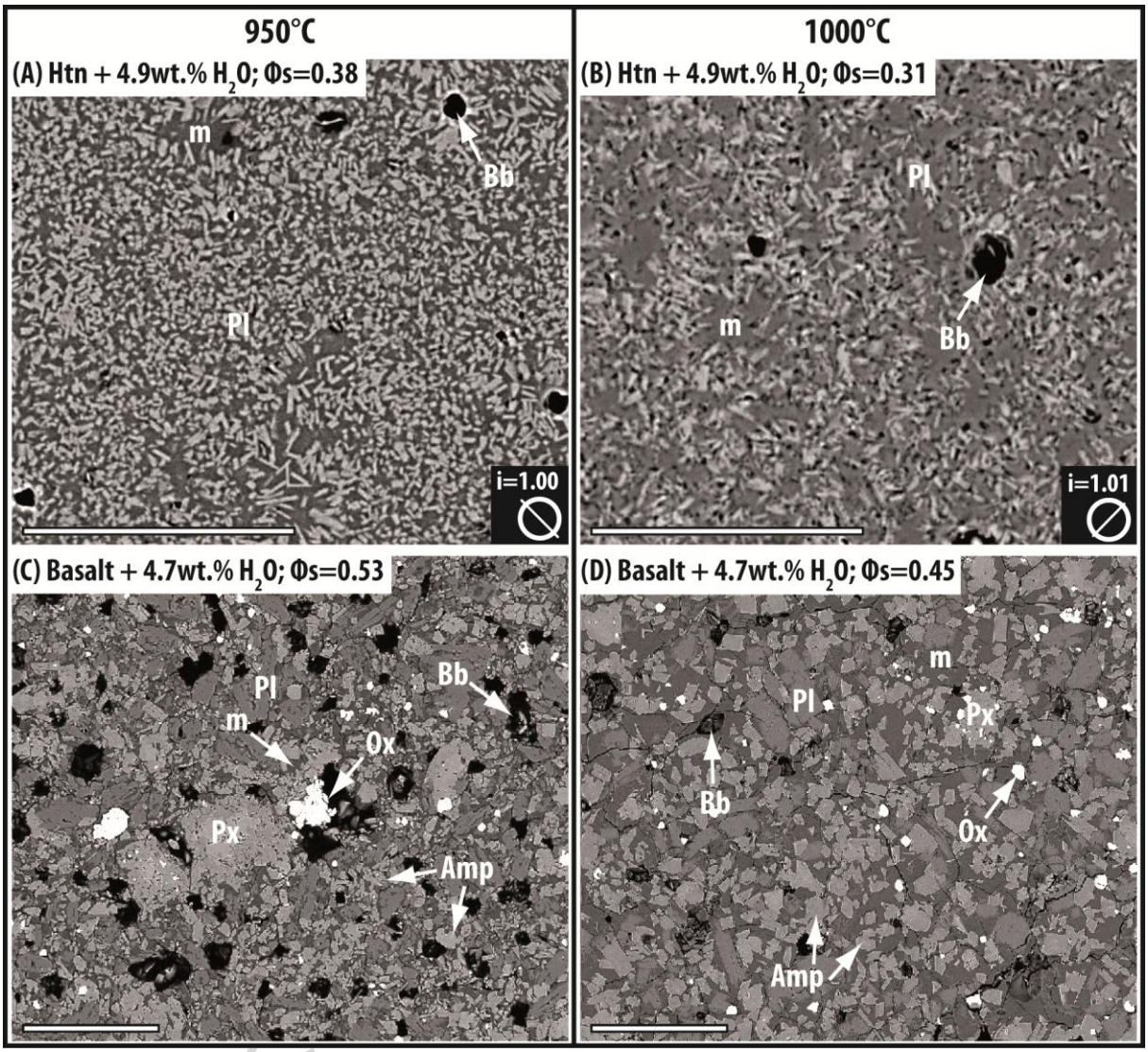

Fig. 2

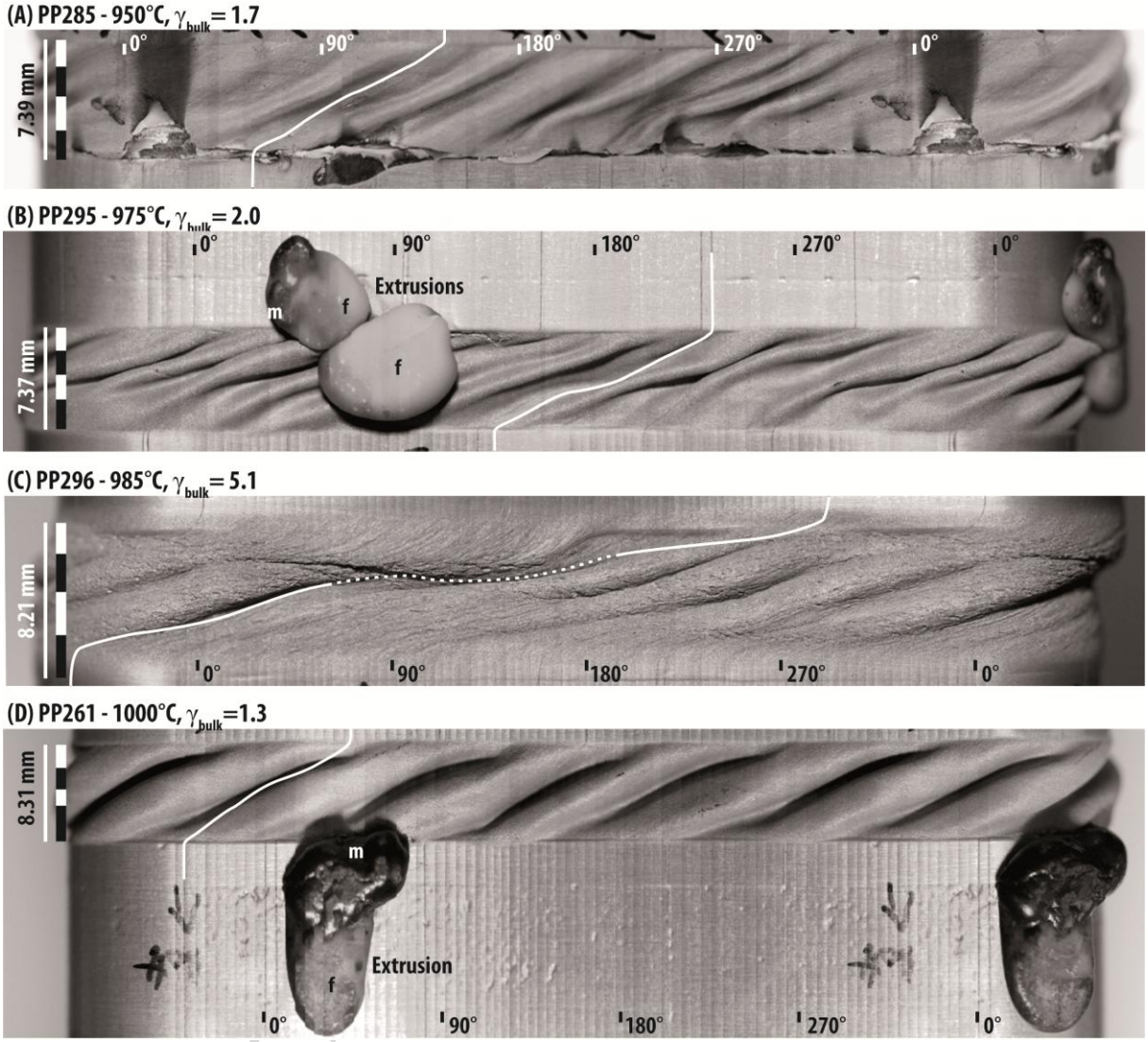

Fig. 3

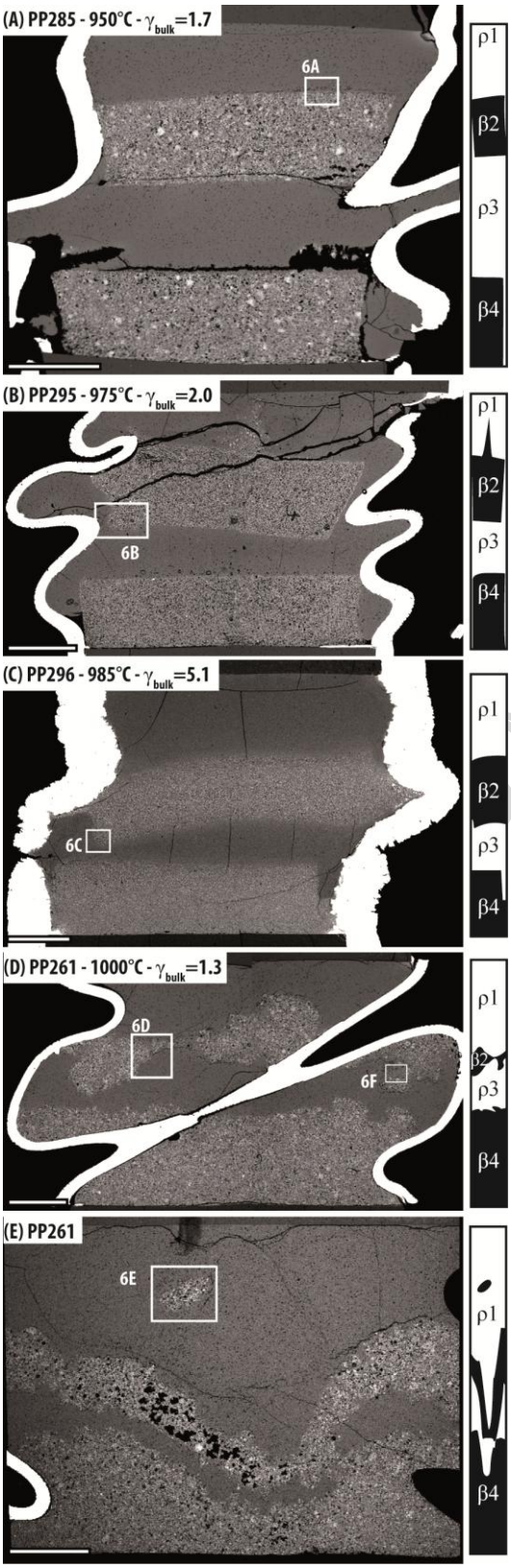

Fig. 4

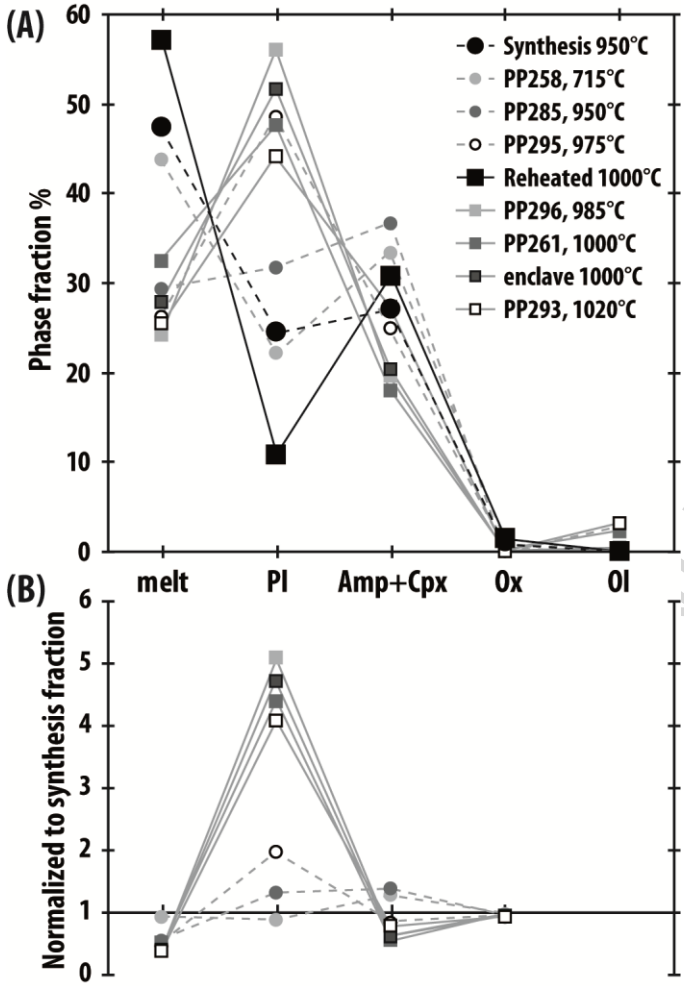

Fig. 5

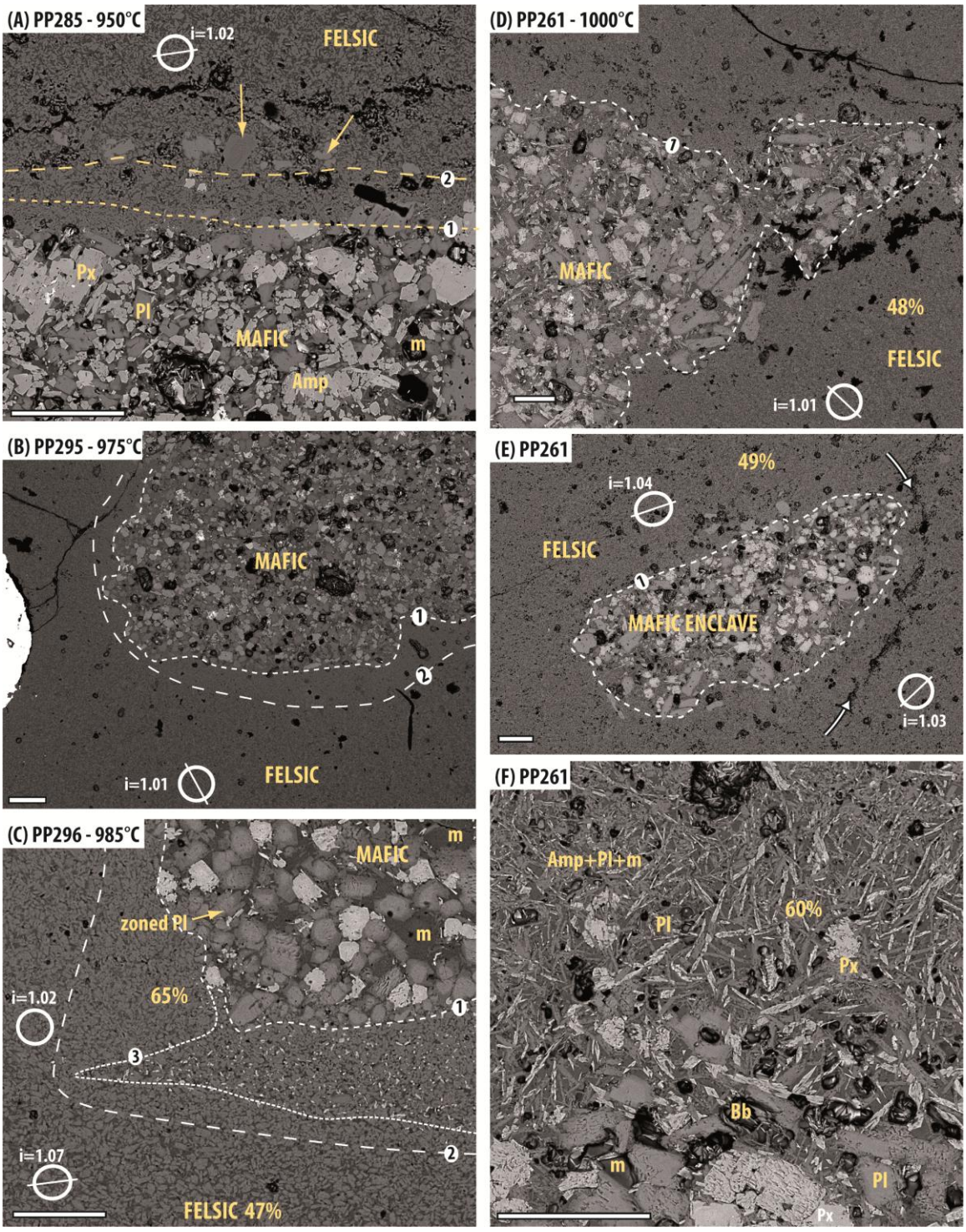

Fig. 6

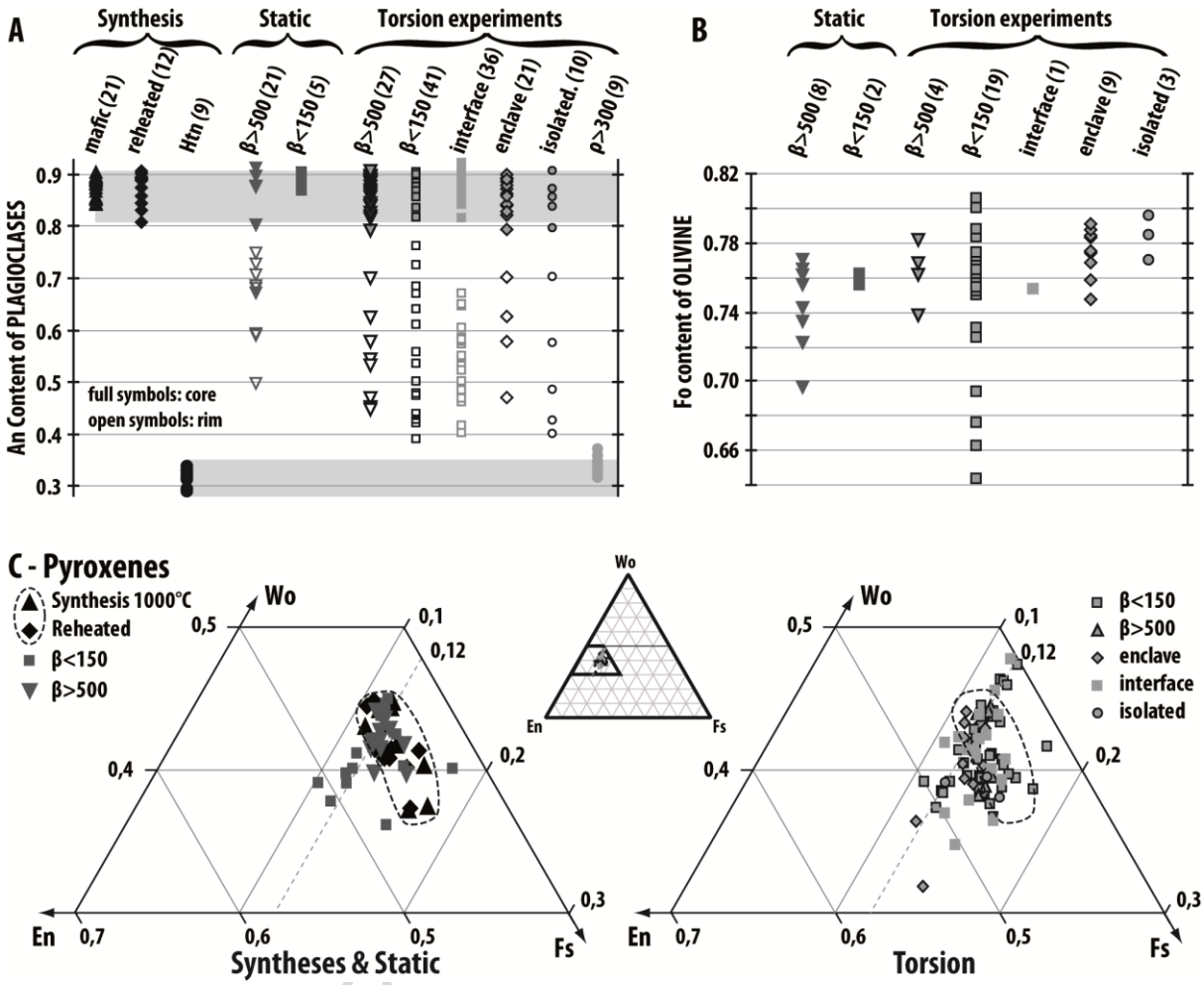

Fig. 7

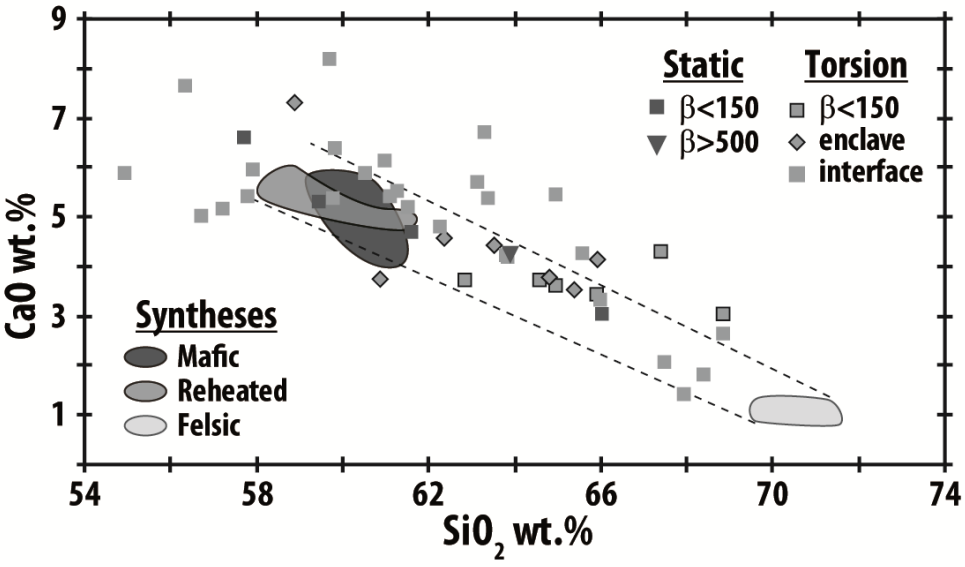

Fig. 8

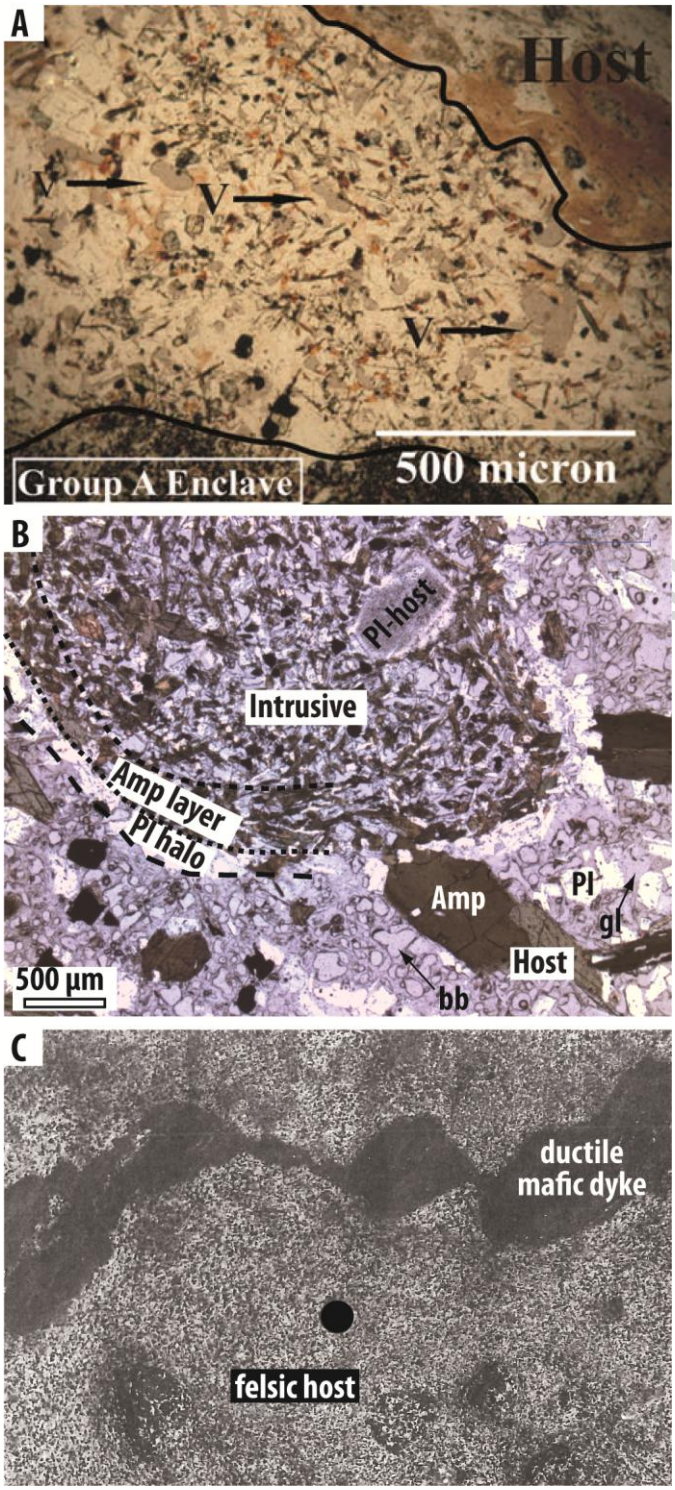

Fig. 9

Table1: Compositions of the starting materials and run products

		SiO_2		TiO_2		Al_2O_3		FeO		MgO		MnO		CaO		Na_2O		K_2O		H_2O		Tot	An	Mg#
Felsic end-member (hydrated haplotonalite)																								
starting	Dry*	68.9				19.6								3.5		8.00						100	0.19	
	Hydrated*	65.5				18.6								3.3		7.61				4.9		100		
Synth. 950	Glass	70.1	*15*	0.03	*4*	15.5	*2*	0.34	*10*	0.00	*1*	0.05	*6*	1.1	*2*	5.4	*14*	0.04	*4*	7.4	*6*	100	0.10	
	Plagioclase	61.6	*12*	0.03	*2*	24.3	*7*	0.13	*8*	0.01	*1*	0.01	*2*	6.3	*4*	7.62	*15*	0.01	*2*			100	0.31	
Synth. 1000	Glass	69.9	*15*	0.02	*4*	15.6	*4*	0.33	*9*	0.00	*1*	0.04	*6*	1.2	*3*	5.7	*14*	0.04	*3*	7.1	*9*	100	0.10	
	Plagioclase	61.4	*14*	0.02	*2*	24.4	*9*	0.09	*9*	0.01	*1*	0.02	*4*	6.4	*5*	7.63	*16*	0.02	*2*			100	0.32	
Mafic end-member (hydrated Santorini basalt)																								
Starting	Dry	50.7		0.91		18.0		9.14		6.72		0.16		11.1		2.80		0.49				100	0.69	0.60
	Hydrated	48.4		0.87		17.2		8.58		6.42		0.15		10.6		2.67		0.47		4.7		100		
Synth. 950	Glass	62.3	*15*	0.45	*11*	18.5	*6*	1.73	*38*	0.4	*3*	0.15	*8*	5.0	*5*	3.8	*8*	1.1	*1*	6.6	*11*	100	0.42	0.32
	Amphibole	43.1	*5*	1.89	*25*	13.2	*4*	10.3	*5*	14.9	*6*	0.19	*12*	12.1	*4*	2.44	*11*	0.27	*5*	1.7	*8*	100		0.75
	Plagioclase	46.1	*8*	0.03	*5*	33.4	*7*	0.9	*2*	0.08	*9*	0.03	*4*	17.9	*7*	1.4	*3*	0.04	*4*			100	0.87	
	Pyroxene	51.7	*11*	0.68	*18*	2.9	*11*	8.6	*9*	15.0	*6*	0.29	*9*	20.6	*10*	0.31	*4*	0.01	*1*			100		0.78
	Oxyde	0.24	*17*	2.47	*1*	6.5	*1*	84.0	*6*	5.78	*12*	0.60	*18*	0.37	*7*	0.00	*0*	0.02	*3*			100		
Synth. 1000	Glass	60.5	*13*	0.40	*15*	18.5	*1*	1.8	*4*	0.39	*13*	0.12	*8*	5.1	*6*	3.8	*2*	1.12	*6*	8.3	*10*	100	An	0.30
	Amphibole	42.5	*12*	1.85	*28*	13.3	*7*	10.3	*4*	15.7	*8*	0.26	*8*	11.7	*5*	2.42	*15*	0.31	*6*	1.7	*6*	100		0.76
	Plagioclase	45.9	*8*	0.02	*2*	33.7	*5*	0.84	*9*	0.03	*2*	0.04	*6*	18.0	*6*	1.4	*2*	0.03	*3*			100	0.87	
	Pyroxene	49.9	*8*	0.75	*20*	3.7	*6*	8.7	*16*	15.7	*5*	0.28	*4*	20.7	*13*	0.34	*7*	0.01	*1*			100		0.79
	Oxyde	0.03	*3*	2.50	*14*	6.2	*2*	84.4	*4*	6.11	*5*	0.54	*10*	0.13	*3*	0.05	*4*	0.01	*1*			100		
1000+ reheated	Glass	59.7	*15*	0.41	*10*	19.2	*5*	2.2	*6*	0.41	*16*	0.20	*10*	5.4	*3*	3.6	*3*	1.03	*13*	7.9	*9*	100	0.45	0.28
	Amphibole	42.4	*9*	1.81	*20*	13.0	*11*	9.7	*5*	16.4	*4*	0.20	*9*	12.2	*12*	2.4	*3*	0.25	*6*	1.7	*8*	10		0.78

																			0		
Plagioclase	45.9	*9*	0.02	*4*	33.9	*6*	0.77	*14*	0.06	*3*	0.05	*5*	17.9	*8*	1.4	*3*	0.03	*4*	100	0.87	
Pyroxene	50.4	*6*	0.78	*12*	3.5	*10*	8.5	*13*	15.8	*4*	0.30	*6*	20.4	*10*	0.36	*6*	0.01	*1*	100		0.79
Oxyde	0.26	*15*	9.6	*21*	2.7	*2*	85.9	*6*	1.00	*10*	0.22	*9*	0.25	*6*	0.00	*1*	0.03	*3*	100		

The felsic Dry* glass is the nominal composition given by Schott, A.G., Hydrated* glass is calculated. Standard deviations in terms of least unit cited are indicated by italic font. Compositions were acquired using a Cameca SX 50 microprobe at 15kV and 6nA. Glass analyses were done with defocused beam (covering an area of ~ 25µm^2) whereas a focused beam (~ 1µm^2) was used for crystal analyses. Glass and minerals are normalized to 100% anhydrous. Water content was calculated by mass difference. Mg# is the molar ratio Mg/(Mg+Fe*) and An is the molar ratio Ca/(Ca+Na).

Table 2: Static and torsion experiments conducted in Paterson apparatus

		Sample										
Exp. N°	T°C Exp.	T°C Synth.	Diam.	Length	ρ1	β2	ρ3	β4	strain rate	Bulk strain	Dur. (h)	Length after Exp.
PP265	600	950	14.96	5.33	2.07	1.16	2.10		2.E-04	0.7	3	5.29
PP258	715	950	14.96	10.93	3.34	1.42	3.27	2.90	5.E-04	1.7	2	10.67
PP285	950	950	14.82	7.39	1.65	1.82	2.08	1.84	5.E-04	1.7	2	7.30
PP295	975	950	14.68	7.37	1.66	1.78	1.78	2.15	2.E-04	2.0	5	7.31
PP296	985	1000	13.78	8.21	1.63	2.06	2.27	2.25	8.E-04	5.1	4	8.19
PP261	1000	1000	14.92	8.31	1.98	1.93	1.39	3.01	3.E-04	1.3	2	8.08
PP293	1020	1000	13.79	8.71	1.50	2.40	2.45	2.36	9.E-04	0.7	2	8.68
PP262	1000	950	14.92	9.12	1.94	2.00	2.03	3.05	0	0	2	9.02

Abbreviations: Exp. N° (experiment number), T°C Exp (experimental temperature in Celsius degrees), T°C Synth. (temperature of synthesis in Celsius degrees), Diam. (diameter), Dur. (duration of the experiment, including equilibration lap time and deformation time). ρ1, β2, ρ3, β4 are the layers composing the sample (see Fig. 1). Dimensions (diameter, initial length, thickness of each layer and length after experiment) are given in mm.

Highlights (mandatory)

We performed the first dynamic mixing experiments between hydrous magmas

Mixing textures are isolated crystals, boudins, enclaves, “diktytaxitic” layers

Mixing of hydrous magmas occurs at T=170°C lower than between similar but dry magmas

Mingling and mixing appears feasible at crystal fraction $\phi < 50$ vol%

Mingling may occur at $\phi > 50$ vol% under higher strain rate conditions (volcanic conduit)